

Vibrational Effects on the F–F Spin–Spin Coupling Constant (${}^2hJ_{\text{F-F}}$) in FHF^- and FDF^- Janet E. Del Bene,^{*,†,‡} Meredith J. T. Jordan,[§] S. Ajith Perera,[‡] and Rodney J. Bartlett[‡]

Department of Chemistry, Youngstown State University, Youngstown, Ohio 44555; Quantum Theory Project, University of Florida, Gainesville, Florida 32611; and School of Chemistry, University of Sydney, Sydney, NSW 2006, Australia

Received: March 22, 2001; In Final Form: June 29, 2001

Calculating F–F spin–spin coupling constants across hydrogen bonds has represented a significant challenge to theory. In this study, ab initio calculations have been carried out to evaluate vibrational effects on the F–F spin–spin coupling constant (${}^2hJ_{\text{F-F}}$) for FHF^- . The coupling-constant surface ${}^2hJ_{\text{F-F}}$ was generated at EOM-CCSD/(qz,p,qz2p), and two-dimensional wave functions for the symmetric and asymmetric stretching vibrations were obtained from the CCSD(T)/aug'-cc-pVTZ potential surface. The effect of the FHF^- bending mode was examined using one-dimensional calculations along the normal coordinate for the bending motion. Although ${}^2hJ_{\text{F-F}}$ is dominated by the Fermi-contact term in the region of the surface surrounding the equilibrium structure, the paramagnetic spin–orbit and spin dipole terms are important in determining the absolute value of ${}^2hJ_{\text{F-F}}$. In the ground vibrational state, the expectation value of the F–F distance increases, and the expectation value of ${}^2hJ_{\text{F-F}}$ decreases to 212.7 Hz, significantly less than the equilibrium value of 254.4 Hz. This decrease is due primarily to a decrease in the expectation value of the Fermi-contact term. The ground-state expectation value of the F–F coupling constant is consistent with an experimental estimate of 220 Hz, obtained by extrapolation of experimental values of ${}^2hJ_{\text{F-F}}$ for larger clusters of $[\text{F}(\text{HF})_n]^-$. For FDF^- , the expectation value of ${}^2hJ_{\text{F-F}}$ in the ground vibrational state is 223.1 Hz. Thermal vibrational averaging at 298 K over lower-energy excited vibrational states has essentially no effect on ${}^2hJ_{\text{F-F}}$.

Introduction

In our first study of X–Y spin–spin coupling constants (${}^2hJ_{\text{X-Y}}$) across X–H–Y hydrogen bonds,¹ we reported ab initio EOM-CCSD F–F coupling constants for the anionic complexes $[\text{F}(\text{HF})_n]^-$, $n = 1-4$. The computed coupling constants were found to be in good agreement with the experimental values without any rescaling of the computed values. This is in contrast to the computed SOS-DFT coupling constants, which had to be rescaled by 210 Hz.² It was also noted¹ that the computed EOM-CCSD coupling constants were always greater than the experimental values, with differences larger than anticipated at this level when compared to coupling constants involving C and N. At that time, we suggested that these differences might well be due to zero-point vibrational effects. Although the F–F coupling constant in FHF^- cannot be measured experimentally, Limbach et al. have estimated a value of approximately 220 Hz from consideration of F–F couplings in $[\text{F}(\text{HF})_n]^-$, for $n > 1$. They also suggested that vibrational averaging may be important in determining ${}^2hJ_{\text{F-F}}$.³ Since there is a difference between correcting for zero-point vibrational effects and vibrational averaging over the vibrational wave functions of all states populated at a given temperature, both will be investigated in this study.

In a previous paper on anharmonicity effects on stretching frequencies, we reported a detailed study of the bihalide ions XHX^- , for X = F, Cl, and Br, and of their deuterated analogues.⁴ In that work, a two-dimensional treatment of vibration in the coordinates $\text{X}_a\text{--H}$ and $\text{X}_b\text{--H}$ was performed, and anharmonic eigenvalues and eigenvectors were obtained. These studies were done at various levels of theory, including CCSD(T)/aug'-cc-pVTZ. At this level, the computed anharmonic frequencies for the symmetric (dimer) and asymmetric (proton)

stretching vibrations of FHF^- are 595 and 1476 cm^{-1} , respectively, in agreement with the gas-phase values of 583 and 1331 cm^{-1} , respectively,⁵ although the computed asymmetric stretching frequency is 145 cm^{-1} higher than the experimental value. For FDF^- , the computed asymmetric stretching frequency is 1023 cm^{-1} , compared to gas-phase and Ar matrix values of 934 and 965 cm^{-1} , respectively.⁵⁻⁷ In the present study, we have used the vibrational wave functions obtained from the CCSD(T)/aug'-cc-pVTZ potential surface for FHF^- and FDF^- to evaluate zero-point and thermal vibrational averaging effects at 298 K on ${}^2hJ_{\text{F-F}}$. We have also examined the effect of the bending mode on ${}^2hJ_{\text{F-F}}$ using a one-dimensional treatment of this vibration. Vibrational effects on NMR properties of some polyatomic molecules have been reported by Oddershede et al.⁸⁻¹⁰

Methods

The structure of FHF^- was optimized using the coupled cluster singles and doubles with noniterative triples [CCSD(T)]^{11,12} level of theory with Dunning's polarized valence triple-split basis set augmented with diffuse functions on F (aug'-cc-pVTZ).¹³⁻¹⁵ A two-dimensional CCSD(T) potential surface was generated in the coordinates $\text{F}_a\text{--H}$ and $\text{F}_b\text{--H}$, and two-dimensional Schrödinger equations were solved to obtain anharmonic eigenvalues and eigenvectors for the symmetric and asymmetric stretching modes of FHF^- and FDF^- . Details concerning the generation of the potential surface and the procedures used to obtain the vibrational eigenfunctions and eigenvalues are reported elsewhere.⁴

A spin–spin coupling-constant surface in the coordinates $\text{F}_a\text{--H}$ and $\text{F}_b\text{--H}$ was computed using the equation-of-motion coupled cluster singles and doubles (EOM-CCSD) method in the CI-like approximation,¹⁶⁻¹⁹ with the (qz,p,qz2p) basis set of Ahlrichs et al.²⁰ Unlike coupling constants ${}^2hJ_{\text{X-Y}}$ across N–H–N, N–H–O, O–H–O, and Cl–H–N hydrogen bonds which are determined solely by the Fermi-contact term,²¹⁻²⁴ ${}^2hJ_{\text{F-F}}$ has nonnegligible contributions from the paramagnetic

[†] Youngstown State University.

[‡] University of Florida.

[§] University of Sydney.

TABLE 1: ${}^{2h}J_{F-F}$ and Components of J as Functions of the F–H Distance in $D_{\infty h}$ Structures of FHF^- ^a

R(F–H)	PSO ^b	DSO ^b	FC ^b	SD ^b	${}^{2h}J_{F-F}$
0.80	-209.3	-1.9	3991.1	1.1	3781.0
0.85	-222.3	-1.6	2914.1	3.0	2693.2
0.90	-228.6	-1.3	2134.8	5.1	1910.0
0.95	-230.0	-1.0	1558.3	8.0	1335.3
1.00	-227.7	-0.8	1129.2	12.0	912.7
1.05	-222.6	-0.7	810.9	17.0	604.6
1.10	-215.4	-0.6	577.2	23.2	384.4
1.15	-206.9	-0.5	407.8	30.5	230.9
1.20	-197.4	-0.4	287.0	38.7	127.9
1.25	-187.4	-0.3	202.2	47.8	62.3
1.30	-177.2	-0.3	143.9	57.9	24.3
1.35	-167.0	-0.2	104.5	68.7	6.0

^a ${}^{2h}J_{F-F}$ and components of J in Hertz; F–H distances in Å. ^b The terms which contribute to the total spin–spin coupling constant are the paramagnetic spin–orbit (PSO), diamagnetic spin–orbit (DSO), Fermi-contact (FC), and spin dipole (SD).

spin–orbit (PSO), Fermi-contact (FC), and spin dipole (SD) terms.^{25–27} Thus, all terms [including the diamagnetic spin–orbit (DSO) term which is very small] were evaluated in order to construct the spin–spin coupling-constant surface. Surfaces for the components of J , except for the diamagnetic spin–orbit surface, were also constructed. The ab initio grid for these surfaces was generated by varying the F_a –H distance from 0.80 to 1.30 Å in steps of 0.10 Å, and then varying the F_b –H distance from the particular value of the F_a –H distance to that distance plus 1.40 Å, in steps of 0.10 Å. The global coupling-constant surfaces were constructed from the ab initio data points analogously to the potential surface. The sensitivity of the calculations to the procedures used to generate these surfaces was examined. The variation in $\langle {}^{2h}J_{F-F} \rangle$ and its components did not exceed 0.01 Hz, a confirmation that the ab initio data points span the appropriate regions. F–H distances and F–F coupling constants in ground and excited vibrational states were computed as expectation values using the vibrational wave functions for FHF^- obtained from the CCSD(T)/aug'-cc-pVTZ potential surface. Distances and coupling constants in the vibrational states of FDf^- were evaluated as expectation values from the vibrational wave functions for this anion. A similar approach for evaluating vibrational effects has been reported in a study of N–N coupling constants in $CNH\cdots NCH$.²⁸

A one-dimensional potential curve and a one-dimensional curve for the F–F spin–spin coupling constant were generated from the normal coordinate vector for the bending mode of FHF^- . The expectation value of J in the ground and lower excited vibrational states of this mode were computed from the corresponding vibrational wave functions.

The data points required to generate the two-dimensional potential surface and the coupling-constant surfaces in the stretching modes, and the one-dimensional potential curve and the corresponding spin–spin coupling-constant curve for the bend mode, were computed using the *ACES II* program.²⁹ These calculations were carried out on the Cray SV1 computer at the Ohio Supercomputer Center and the computing facilities at the University of Sydney.

Results and Discussion

Table 1 presents values of the paramagnetic spin–orbit, diamagnetic spin–orbit, Fermi-contact, and spin dipole terms, as well as total ${}^{2h}J_{F-F}$, for FHF^- structures with $D_{\infty h}$ symmetry as a function of the F–H distance. Figure 1 presents a plot of the Fermi-contact term and ${}^{2h}J_{F-F}$ along cuts through the Fermi-contact and coupling-constant surfaces that correspond to structures with $D_{\infty h}$ symmetry. It is apparent from Table 1 and

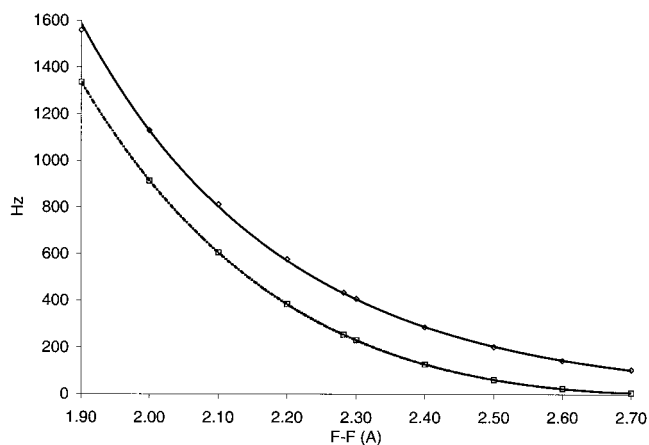


Figure 1. Fermi-contact term (\diamond) and ${}^{2h}J_{F-F}$ (\square) plotted against the F–F distance for structures with $D_{\infty h}$ symmetry.

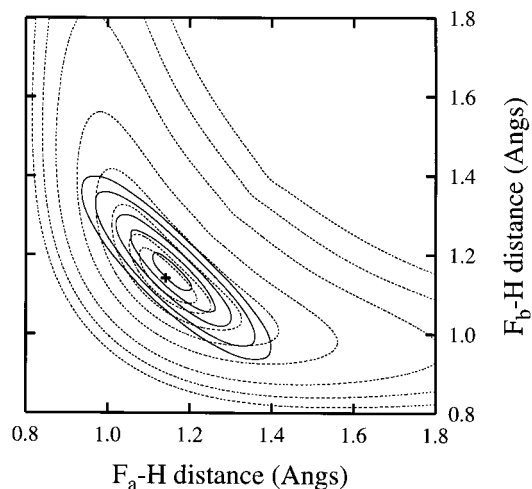


Figure 2. Square of the ground-state vibrational wave function superimposed on the CCSD(T)/aug'-cc-pVTZ potential surface, taken from an earlier study.⁴ Contours are at 0.0005, 0.001, 0.0025, 0.005, 0.01, 0.02, 0.03, and 0.04 E_h above the global minimum energy. The cross corresponds to the equilibrium structure.

Figure 1 that ${}^{2h}J_{F-F}$ is determined primarily by the Fermi-contact term, although both the paramagnetic spin–orbit and spin dipole terms are important for determining the absolute value of ${}^{2h}J_{F-F}$. What is also apparent from Figure 1 is that at very short F–F distances including the region surrounding the equilibrium structure, the Fermi-contact term is extremely large and changes approximately exponentially with F–F distance. As a result, the computed spin–spin coupling constant for the equilibrium structure is very sensitive to the F–F distance. For the equilibrium structure, $R_e(F-F)$ is 2.282 Å, and ${}^{2h}J_{F-F}$ has a value of 254.4 Hz.

Figures 2 and 3 present plots of the square of the ground-state vibrational wave function superimposed on the potential-energy surface and the coupling-constant surface, respectively. In both figures, the equilibrium structure is represented by a cross. The anion FHF^- is tightly bound, with a CCSD(T)/aug'-cc-pVTZ binding energy of -44.6 kcal/mol relative to HF and F^- . The equilibrium F–F distance in FHF^- is short, and as is evident from Figure 2, the repulsive walls on the potential surface are very steep. This pushes the wave function to larger H–F and F–F distances than the equilibrium values, as evident from both Figures 2 and 3. What is crucial is the extremely large magnitude of the Fermi-contact term at short F–F distances. Any shift to longer distances causes a large decrease in the value of the Fermi-contact term and a correspondingly

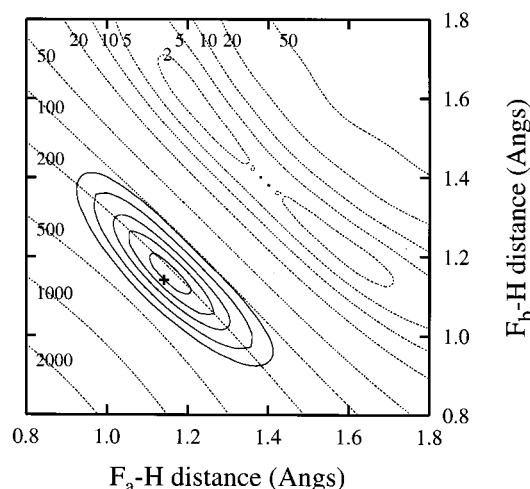


Figure 3. Square of the ground-state vibrational wave function superimposed on the ${}^{2h}J_{F-F}$ surface. The cross corresponds to the equilibrium structure. Contour values, in Hertz, are indicated. Over the range of chemical interest, ${}^{2h}J_{F-F}$ decreases with increasing F–F distance. At larger distances, it increases as the spin–dipole term dominates. At very large distances, ${}^{2h}J_{F-F}$ goes to zero.

TABLE 2: Properties of FHF[−] in Ground and Excited Vibrational States^a

state ^b	frequency	<H–F> ^c	PSO ^d	FC ^d	SD ^d	< ${}^{2h}J_{F-F}$ > ^e
Ground and Excited Vibrational States of the Symmetric Stretching Mode						
(0,0)		1.158	−196.4	380.5	29.1	212.7
(1,0)	594.9	1.165	−194.3	377.7	29.9	212.8
(2,0)	1179.7	1.171	−191.8	374.2	30.5	212.4
(3,0)	1753.1	1.178	−188.9	369.0	31.1	210.8
(4,0)	2311.1	1.186	−185.1	362.0	31.5	207.9
(5,0)	2849.9	1.196	−180.2	351.9	31.5	202.7
Excited Vibrational States of the Asymmetric Stretching Mode						
(0,1)	1476.0	1.190	−175.0	291.9	28.2	144.7
Excited Vibrational States in which Both Modes Are Excited						
(1,1)	2006.6	1.198	−171.9	288.5	28.6	144.8
(2,1)	2524.8	1.205	−168.5	284.4	28.9	144.3
At Equilibrium						
	$R_e(H-F)$	PSO	FC	SD	${}^{2h}J_{F-F}$	
	1.141	−208.5	434.3	29.1	254.4	

^a Frequencies in inverse centimeters; distances in angstroms; J and components of J in Hertz. ^b The notation (i,j) indicates i quanta of energy in the symmetric stretch and j quanta of energy in the asymmetric stretch. ^c The expectation value of the H–F distance. ^d The expectation values of the components of J . See Table 1. ^e The <DSO> is approximately −0.5 Hz in all cases.

large decrease in ${}^{2h}J_{F-F}$. This can be seen from the data of Table 2. At the equilibrium F–F distance of 2.282 Å, the Fermi-contact term is 434.3 Hz, the paramagnetic spin–orbit term is −208.5 Hz, and ${}^{2h}J_{F-F}$ is 254.4 Hz. In the ground vibrational state [the (0,0) state in Table 2], the expectation value of the F–F distance increases to 2.316 Å, the paramagnetic spin–orbital term increases by 12.1 Hz, but the Fermi-contact term decreases by 53.8 Hz. As a result, $\langle {}^{2h}J_{F-F} \rangle$ decreases by 41.7 Hz to 212.7 Hz. This rather dramatic change in the coupling constant does, indeed, account for the difference between the computed F–F coupling constant for the equilibrium structure of FHF[−] and the experimental estimate of Limbach et al. of about 220 Hz. The value of ${}^{2h}J_{F-F}$ interpolated from the coupling-constant surface at F–H bond lengths of 1.158 Å is 211.4 Hz, within 1% of the expectation value.

What effect does vibrational averaging at 298 K have on the value of ${}^{2h}J_{F-F}$? Table 2 reports expectation values of the H–F distance and total J and components of J in lower-energy

vibrational states of FHF[−]. Excitation of the symmetric stretching mode (the F–F stretch) leads to increases in the expectation value of the F–F distance, as expected. In Figure 3, this mode corresponds to motion along the diagonal which maintains $D_{\infty h}$ symmetry. As apparent from Table 2, there is little change in $\langle {}^{2h}J_{F-F} \rangle$ in the low-energy excited states of the symmetric stretching mode. Although the Fermi-contact term decreases as $\langle F-H \rangle$ increases, this decrease is balanced by increases in the paramagnetic spin–orbit and spin dipole terms. Moreover, the lower-energy vibrational states of FHF[−] are relatively high in energy compared to the dimer vibrational states of other hydrogen-bonded complexes. As a result, they are not significantly populated at room temperature, and vibrational averaging has essentially no effect on ${}^{2h}J_{F-F}$. This result is in contrast to the results of our study of zero-point and vibrational averaging effects at 298 K in CNH \cdots NCH, where thermal vibrational averaging was found to be important in determining ${}^{2h}J_{N-N}$.²⁸

It is apparent from Table 2 that $\langle {}^{2h}J_{F-F} \rangle$ decreases significantly in the first excited state of the asymmetric (proton) stretch. Excitation of this mode leads to a large increase in $\langle H-F \rangle$ and produces a structure with a proton-shared but not symmetric hydrogen bond.^{30,31} We have already observed that complexes with symmetric hydrogen bonds have larger coupling constants than corresponding complexes in which the hydrogen bond is proton-shared but not symmetric.^{21–24} Thus, in the first excited state of the asymmetric stretch, $\langle H-F \rangle$ increases by 0.032 Å relative to the ground vibrational state, the Fermi-contact term decreases by 89 Hz, but the paramagnetic spin–orbit term increases by only 21 Hz. As a result, $\langle {}^{2h}J_{F-F} \rangle$ decreases to 144.7 Hz. Because the first excited vibrational state of the asymmetric stretch is 1476 cm^{−1} above the ground state, vibrational averaging at 298 K has essentially no effect on ${}^{2h}J_{F-F}$.

The third vibrational mode in FHF[−] is the doubly degenerate bending mode. Because of the large difference in mass between hydrogen and fluorine atoms, the bending vibration principally involves motion of the hydrogen atom, and there is very little change in the F–F distance. Indeed, in the harmonic approximation, the F–F distance remains constant. As a result, the bending motion is expected to have little effect on the value of ${}^{2h}J_{F-F}$. This is confirmed by one-dimensional calculations carried out along the normal mode displacement vector for the bending motion. In the ground vibrational state of the bending mode, $\langle {}^{2h}J_{F-F} \rangle$ is 253.2 Hz, very similar to the equilibrium value of 254.4 Hz. The expectation values of the coupling constant decrease slightly in the excited states of the bending mode. For example, $\langle {}^{2h}J_{F-F} \rangle$ for the first and second excited states of this mode are 250.8 and 248.3 Hz, respectively. However, because the bending mode is also a relatively high frequency vibration, vibrational averaging at 298 K has essentially no effect on ${}^{2h}J_{F-F}$.

Table 3 presents anharmonic symmetric and asymmetric stretching frequencies, $\langle D-F \rangle$, and $\langle {}^{2h}J_{F-F} \rangle$ for FDF[−]. The $\langle F-F \rangle$ in the ground vibrational state of FDF[−] is 2.310 Å, which is, as expected, slightly shorter than the distance of 2.316 Å in FHF[−]. As a result, $\langle {}^{2h}J_{F-F} \rangle$ in the ground vibrational state of FDF[−] is 223.1 Hz, 10.4 Hz greater than the ground-state value for FHF[−], but significantly less than the value of 254.4 Hz for the equilibrium structure. Deuterium substitution has only a small effect on the frequencies of the symmetric stretch, but a much larger effect on the asymmetric stretching frequencies, as seen in Table 3. However, the excited states are still relatively high in energy, and vibrational averaging over

TABLE 3: Properties of FDF⁻ in Ground and Excited Vibrational States^a

state ^b	frequency	<D-F> ^c	< ^{2h} J _{F-F} >
Ground and Excited Vibrational States of the Symmetric Stretching Mode			
(0,0)		1.155	223.1
(1,0)	600.5	1.160	222.6
(2,0)	1188.3	1.167	221.0
(3,0)	1758.3	1.176	216.2
(4,0)	2310.2	1.187	203.0
Excited Vibrational States of the Asymmetric Stretching Mode			
(0,1)	1022.6	1.177	168.4
(0,2)	2198.8	1.194	141.6
Excited Vibrational States in which Both Modes Are Excited			
(1,1)	1568.9	1.185	167.4
(2,1)	2100.0	1.194	165.6
(3,1)	2613.7	1.203	162.8

^a Frequencies in inverse centimeters; distances in angstroms; and *J* in Hertz. ^b The notation (*i,j*) indicates *i* quanta of energy in the symmetric stretch and *j* quanta of energy in the asymmetric stretch. ^c Expectation value of the D–F distance.

these states at 298 K has essentially no effect on the value of the F–F coupling constant in FDF⁻.

Conclusions

In this study, vibrational effects on the F–F spin–spin coupling constant (^{2h}J_{F–F}) in FHF⁻ and FDF⁻ have been evaluated from the EOM-CCSD/(qzp,qz2p) coupling-constant surface using vibrational wave functions obtained for these anions from the CCSD(T)/aug'-cc-pVTZ potential surface. The following statements are supported by these calculations.

(1) Relative to the equilibrium F–F distance, the expectation value of this distance increases in the ground vibrational state and in the excited vibrational states of the symmetric (dimer) and asymmetric (proton) stretching modes.

(2) In the region of the equilibrium structure, the F–F distance is very short, and ^{2h}J_{F–F} is dominated by the Fermi-contact term, although both the paramagnetic spin–orbit and spin dipole terms are important in determining the absolute value of ^{2h}J_{F–F}.

(3) In the ground vibrational state of FHF⁻, the expectation value of the F–F distance increases, and ^{2h}J_{F–F} decreases from its equilibrium value of 254.4 Hz to 212.7 Hz. This value of the coupling constant is in reasonable agreement with an extrapolated experimental value of about 220 Hz.

(4) In the excited vibrational states of the symmetric stretching mode, the expectation value of the F–F distance increases, but the expectation value of ^{2h}J_{F–F} is essentially unchanged. This is the result of a cancellation due to a decrease in the expectation value of the Fermi-contact term and increases in the expectation values of the paramagnetic spin–orbit and spin dipole terms.

(5) In the first excited state of the asymmetric stretching mode, the expectation value of the F–F distance increases and the expectation value of ^{2h}J_{F–F} decreases dramatically as the hydrogen bond is no longer symmetric. This state lies relatively high in energy above the ground vibrational state. Thermal vibrational averaging at 298 K over all of the lower-energy excited states of both stretching modes leaves ^{2h}J_{F–F} essentially unchanged.

(6) The FHF⁻ bending motion has little effect on ^{2h}J_{F–F}. In the ground state of the bend, ^{2h}J_{F–F} decreases from 254.4 to 253.2 Hz. Although ^{2h}J_{F–F} decreases as the bending mode is excited, the excited vibrational states are relatively high in

energy, and thermal vibrational averaging at 298 K leaves ^{2h}J_{F–F} essentially unchanged.

(7) The expectation value of the F–F coupling constant in the ground vibrational state of FDF⁻ is also significantly less than the equilibrium value, but larger than the ground-state coupling constant of FHF⁻. Vibrational averaging at 298 K over low-energy excited vibrational states of FDF⁻ also has essentially no effect on ^{2h}J_{F–F}.

Acknowledgment. This work was supported by grants from the National Science Foundation (CHE-9873815), the Australian Research Council (A1466), and the Air Force Office of Scientific Research (AFO-F49620-98-1-0477). Thanks are also due to the Ohio Supercomputer Center for continuing computational support.

References and Notes

- Perera, S. A.; Bartlett, R. J. *J. Am. Chem. Soc.* **2000**, *122*, 1231.
- Shenderovich, I. G.; Smirnov, S. N.; Denisov, G. S.; Gindin, V. A.; Golubev, N. S.; Dunger, A.; Reibke, R.; Kirpekar, S.; Malkina, O. L.; Limbach, H.-H. *Ber. Bunsenges. Phys. Chem.* **1998**, *102*, 422.
- Benedict, H.; Shenderovich, I. G.; Malkina, O. L.; Malkin, V. G.; Denisov, G. S.; Golubev, N. S.; Limbach, H.-H. *J. Am. Chem. Soc.* **2000**, *122*, 1979.
- Del Bene, J. E.; Jordan, M. J. T. *Spectrochim. Acta* **1999**, *A55*, 719.
- Kawaguchi, K.; Hirota, E. *J. Chem. Phys.* **1987**, *87*, 6838.
- Hunt, R. D.; Andrews, L. *J. Chem. Phys.* **1987**, *87*, 6819.
- McDonald, S. A.; Andrews, L. *J. Chem. Phys.* **1979**, *70*, 3134.
- Oddershede, J.; Geertsen, J.; Scuseria, G. E. *J. Phys. Chem.* **1988**, *92*, 3056.
- Geertsen, J.; Oddershede, J.; Raynes, W. T.; Scuseria, G. E. *J. Magn. Reson.* **1991**, *93*, 458.
- Geertsen, J.; Oddershede, J.; Raynes, W. T. *Magn. Reson. Chem.* **1993**, *31*, 722.
- Bartlett, R. J. In *Modern Electronic Structure Theory: Part I*; Yarkony, D. R., Ed.; World Scientific Publishing Co.: Singapore, 1995, and references therein.
- Bartlett, R. J. *J. Phys. Chem.* **1989**, *93*, 1989 and references therein.
- Dunning, T. H., Jr. *J. Chem. Phys.* **1989**, *90*, 1007.
- Kendall, R. A.; Dunning, T. H., Jr.; Harrison, R. J. *J. Chem. Phys.* **1992**, *96*, 6796.
- Woon, D. E.; Dunning, T. J., Jr. *J. Chem. Phys.* **1993**, *98*, 1358.
- Perera, S. A.; Sekino, H.; Bartlett, R. J. *J. Chem. Phys.* **1994**, *101*, 2186.
- Perera, S. A.; Nooijen, M.; Bartlett, R. J. *J. Chem. Phys.* **1996**, *104*, 3290.
- Perera, S. A.; Bartlett, R. J. *J. Am. Chem. Soc.* **1995**, *117*, 8476.
- Perera, S. A.; Bartlett, R. J. *J. Am. Chem. Soc.* **1996**, *118*, 7849.
- Schafer, A.; Horn, H.; Ahlrichs, R. *J. Chem. Phys.* **1992**, *97*, 2571.
- Del Bene, J. E.; Perera, S. A.; Bartlett, R. J. *J. Am. Chem. Soc.* **2000**, *122*, 3560.
- Del Bene, J. E.; Jordan, M. J. T. *J. Am. Chem. Soc.* **2000**, *122*, 4794.
- Del Bene, J. E.; Perera, S. A.; Bartlett, R. J. *J. Phys. Chem. A* **2001**, *105*, 930.
- Del Bene, J. E.; Bartlett, R. J. *J. Am. Chem. Soc.* **2000**, *122*, 10480.
- Ramsey, N. F. *Phys. Rev.* **1953**, *91*, 303.
- Fukui, H. *Prog. NMR Spectrosc.* **1999**, *35*, 267.
- Helgaker, T.; Jazunski, M.; Rudd, K. *Chem. Rev.* **1999**, *99*, 293.
- Jordan, M. J. T.; Toh, J. S.-S.; Del Bene, J. E. *Chem. Phys. Lett.* submitted for publication.
- Stanton, J. F.; Gauss, J.; Watts, J. D.; Nooijen, M.; Oliphant, N.; Perera, S. A.; Szalay, P. G.; Lauderdale, W. J.; Gwaltney, S. R.; Beck, S.; Balkova, A.; Bernholdt, D. E.; Baeck, K.-K.; Rozyczko, P.; Sekino, H.; Huber, C.; Bartlett, R. J. *ACES-II Quantum Theory Project, University of Florida*. Integral packages included are *VMOL* (Almlöf, J.; Taylor, P. R.), *VPROPS* (Taylor, P. R.), and *ABACUS* (Helgaker, T.; Jensen, H. J. Aa.; Jorgensen, P.; Olsen, J.; Taylor, P. R.).
- Del Bene, J. E.; Jordan, M. J. T. *Int. Rev. Phys. Chem.* **1999**, *18*, 119.
- Jordan, M. J. T.; Del Bene, J. E. *J. Am. Chem. Soc.* **2000**, *122*, 2101.